Supporting Information:

One-Step Facile Surface Engineering of Hydrophobic Nanocrystals with Designer Molecular Recognition

Tao Chen, Ismail Öçsoy, Quan Yuan, Ruowen Wang, Mingxu You, Zilong Zhao, Erqun Song, Xiaobing Zhang and Weihong Tan*

Center for Research at Bio/Nano Interface, Department of Chemistry and Department of Physiology and Functional Genomics, Shands Cancer Center, UF Genetics Institute and McKnight Brain Institute, University of Florida, Gainesville, Florida 32611-7200; Molecular Science and Biomedicine Laboratory, State Key Laboratory of Chemo/Bio-Sensing and Chemometrics, College of Biology and College of Chemistry and Chemical Engineering, Hunan University, Changsha, 410082

*Address correspondence to tan@chem.ufl.edu

1. Synthesis and characterization of hydrophobic nanocrystals

1.1 Synthesis of hydrophobic nanocrystals

1.1.1. Synthesis of 13-nm Fe-Fe_3O_4 core-shell magnetic nanoparticles (CSNPs)

The 13-nm Fe-Fe_3O_4 CSNPs were synthesized using a modified protocol[1,2] Oleylamine (0.3 mL, 0.9 mmol) was mixed with 20 mL 1-octadecene. The mixture was heated to 120 ˚C and degassed under argon at that temperature for 30 min to remove moisture and oxygen. Then, the temperature of the mixture was further increased to 180 ˚C, and 0.7 mL $Fe(CO)_5$ was quickly injected into the mixture with vigorous stirring under argon. The mixture was kept at 180 ˚C for 30 min and then cooled to room temperature before being exposed to air. After discarding the supernatant, the Fe-Fe_3O_4 CSNPs coated on the magnetic stirring bar were transferred to a centrifuge vial and washed with hexane in the presence of oleylamine. After addition of isopropanol, the precipitated Fe-Fe_3O_4 CSNPs

were collected by centrifugation at 12,000 rpm for 20 min. After repeating this procedure 3 times, the purified Fe-Fe_3O_4 CSNPs were dispersed in hexane with 40 μL oleylamine and stored at 4 ˚C for future use.

Since the amorphous Fe_3O_4 shell of the as-synthesized nanoparticles is not stable in dispersion state, it was further oxidized to produce a stable crystalline Fe_3O_4 shell using an oxygen transferring reagent. Five mg $(CH_3)_3NO$ was mixed with 20 mL 1-octadecene. The mixture was heated to 130 ˚C and degassed under argon at that temperature for 30 min to remove moisture and oxygen. Then, 80 mg as-synthesized nanoparticles dispersed in 2 mL hexane were quickly injected into the mixture with vigorous stirring under argon, and the resultant mixture was kept at 130 ˚C for another 2 h to remove hexane. The solution was then heated to 250 ˚C, kept at that temperature for 30 min, and then cooled to room temperature before being exposed to air. After adding isopropanol, the stabilized Fe-Fe_3O_4 CSNPs as a black precipitate were collected by centrifuge at 12,000 rpm for 20 min. The collected Fe-Fe_3O_4 CSNPs were then dispersed in hexane and precipitated by adding isopropanol. After repeating this procedure 3 times, the purified Fe-Fe_3O_4 CSNPs were dispersed in hexane with 40 μL oleylamine and stored at 4 ˚C for future use.

1.1.2. Synthesis of 7-nm Fe_3O_4 nanoparticles (NPs)

The 7-nm Fe_3O_4 NPs were synthesized using a modified protocol.[3] $Fe(acac)_3$ (0.71 g, 2 mmol), 2 mL oleic acid (~6 mmol) and 2 mL oleylamine (~4 mmol) were mixed with 20 mL phenyl ether under argon with vigorous stirring. Then 2.58 g 1,2-hexadecanediol (10 mmol) was added, and the mixture was refluxed at 265 ˚C for 2h. The mixture was cooled to room temperature before being exposed to air. After adding ethanol, the Fe_3O_4 NPs as a black precipitate were collected by centrifuging at 12,000 rpm for 20 min. The

collected Fe_3O_4 NPs were then dispersed in hexane and precipitated by adding ethanol. After repeating this procedure 3 times, the purified Fe_3O_4 NPs were dispersed in hexane with 40 μL oleylamine and stored at 4 ˚C for future use.

1.1.3. Synthesis of 15-nm Fe_3O_4 nanoparticles (NPs)

The 15-nm Fe_3O_4 NPs were provided as a generous gift from Tie Wang in the laboratory of Dr. Charles Cao, Department of Chemistry, University of Florida.

1.1. 4. Synthesis of 13-nm Au nanoparticles (Au NPs)

The 13-nm Au NPs were synthesized using a modified protocol.[4] $HAuCl_4 \cdot 3H_2O$ (0.196 g, 0.5 mmol) and 1.5 ml oleylamine (~3 mmol) were mixed with 10 mL phenyl ether. After the addition of 0.516 g 1,2-hexadecanediol (2 mmol), the temperature of the mixture was slowly increased to 185 ˚C and kept at that temperature for 1.5 h under argon. The mixture was cooled to room temperature before being exposed to air. After adding ethanol, the precipitated Au NPs were collected by centrifugation at 12,000 rpm for 20 min. The collected Au NPs were then dispersed in hexane and precipitated by adding ethanol. After repeating this procedure 3 times, the purified Au NPs were dispersed in hexane with 40 μL oleylamine and stored at 4 ˚C for future use.

1.1.5. Synthesis of 6-nm CdS/ZnS quantum dots (QDs)

The 3-nm CdS/ZnS QDs were synthesized using a modified protocol.[5] Cadmium myristate (1.0 mmol) and sulfur (0.5 mmol) were mixed with 50 g of 1-octadecene. The mixture was degassed at room temperature and then heated to 240 ˚C under argon. The nanocrystal growth was monitored using UV-Vis spectroscopy. When the nanocrystal size reached 3.1 nm in diameter, the mixture was cooled to room temperature. After adding acetone, the precipitated CdS NPs were collected by centrifuging at 14,000 rpm

for 30 min and redispersed in toluene. ZnS shells were grown onto the as-synthesized CdS NPs in a mixture of 1-octadecence and oleylamine (volume ratio of 3:1). Zinc stearate in 1-octadecene (40 mM) and oleylamine (40 mM) in 1-octadecene were injected alternatively with a growth time of 10 min after each injection. As soon as the desired shell thickness was achieved, as calculated by the method of Mews,[6] the mixture was cooled to room temperature. After adding acetone, the precipitated CdS/ZnS QDs were collected by centrifugation at 14,000 rpm for 30 min. The collected CdS/ZnS QDs were then dispersed in hexane and precipitated by adding ethanol. After repeating this procedure 3 times, the purified CdS/ZnS QDs were dispersed in hexane with 40 μL oleylamine and stored at 4 ˚C for future use.

1.1.6. Synthesis of Fe-Pt nanorods (NRs)

Fe-Pt NRs were synthesized using a modified protocol.[7] $Pt(acac)_2$ (49.2 mg, 0.125 mmol), 50 mg 1,2-hexadecanediol (0.2 mmol), and 6 mL oleylamine (~12 mmol) were mixed with 2 mL octyl ether. The mixture was stirred vigorously under argon. Then the temperature of the mixture was increased to 100˚C and kept at that temperature for 20 min to remove moisture and oxygen. Then, $Fe(CO)_5$ (0.025 mmol) was quickly injected into the mixture. After another 20 min, 3 ml oleylamine (~6 mmol) was quickly injected into the mixture. The temperature of the mixture was increased to 300 ˚C and kept at that temperature for 1.5 h. The mixture was cooled to room temperature before being exposed to air. After adding ethanol, the precipitated Fe-Pt NRs were collected by centrifuging at 6000 rpm for 20 min. The collected Fe-Pt NRs were then dispersed in hexane and precipitated by adding ethanol. After repeating this procedure 3 times, the purified NRs were dispersed in hexane with 40 μL oleylamine and stored at 4 ˚C for future use.

1.1.7. Synthesis of Au-Fe_3O_4 dimer nanoparticles (DNPs)

Au-Fe_3O_4 DNPs were synthesized using a modified protocol.[8] $HAuCl_4 \cdot 3H_2O$ (0.1 g, 0.25 mmol) and 10 mL oleylamine (~20 mmol) were mixed with 10 mL tetralin at room temperature and initially stirred for 10 min. Tetra-*n*-butylammonium bromide (TBAB) (1 mmol) and 1 mL oleylamine (~2 mmol) were mixed with 1 mL tetralin by sonication and quickly injected into the above solution. The mixture was further stirred at room temperature for 1 h. After adding ethanol, the precipitated Au NP seeds were collected by centrifuging at 14,000 rpm for 20 min. The collected Au NP seeds were then dispersed in hexane and precipitated by adding ethanol. After repeating this procedure 3 times, the purified Au NP seeds were dispersed in hexane with 40 μL oleylamine and stored at 4 ˚C for future use.

Ten mg as-synthesized Au NP seeds (4 nmol) dissolved in 1 mL hexane, 0.5 mL oleylamine (~1 mmol) and 1 mL oleic acid (~3 mmol) were mixed with 10 mL 1-octadecene. The temperature of the mixture was increased to 120 ˚C and kept at that temperature for 20 min under gentle argon flow to remove hexane. Then 50 μL $Fe(CO)_5$ was quickly injected into the mixture under argon. The temperature of the mixture was further increased to 310˚C and was kept at that temperature for 30 min. The mixture was cooled to room temperature before being exposed to air. After adding isopropanol, the precipitated Au-Fe_3O_4 DNPs were collected by centrifuging at 12,000 rpm for 20 min. The collected Au-Fe_3O_4 DNPs were then dispersed in hexane and precipitated by adding isopropanol. After repeating this procedure 3 times, the purified Au-Fe_3O_4 DNPs were dispersed in hexane with 40 μL oleylamine and stored at 4˚C for future use.

1.2. Transmission electron microscopy (TEM) images of hydrophobic nanocrystals

TEM images were obtained on a Hitachi H-7000 transmission electron microscope at 100 kV. Five-μL samples of hydrophobic nanocrystals in their hydrophobic solvents were dropped onto 3 mm copper grids covered with a continuous carbon film. The samples were air-dried at room temperature.

2. Synthesis and characterization of amphiphilic oligonucleotides

All amphiphilic oligonucleotide sequences were synthesized on the ABI 3400 DNA/RNA synthesizer (Applied Biosystems, Foster City, CA, USA) on a 1.0 micromolar scale using the corresponding controlled pore glass (CPG). As-synthesized diacyllipid phosphoramidite[9] was dissolved in dichloromethane to a concentration of 0.1 M and then coupled using the DNA synthesizer. Detailed sequence information for all the amphiphilic oligonucleotides is provided in Table S1. After the synthesis, the amphiphilic oligonucleotides were cleaved and deprotected from the CPG in 3 mL AMA solution (ammonium hydroxide : 40% aqueous methylamine = 1:1) at 65 ˚C for 25 min. All deprotected sequences were precipitated by adding 250 μL 3M NaCl and 6 mL cold ethanol and collected by centrifuging at 4,000 rpm for 30 min. After dissolving in 200 μL triethylammonium acetate (TEAA), amphiphilic oligonucleotide sequences were purified by reverse phase high pressure liquid chromatography (ProStar, Varian, Walnut Creek, CA, USA) using a C4 column (BioBasic-4, 200 mm x 4.6 mm, Thermo Scientific, USA) with 0.1 M TEAA and acetonitrile as the eluent. Finally, the purified amphiphilic oligonucleotide sequences were quantified by measuring their absorbances at 260 nm on a Cary Bio-100 UV spectrometer (Varian, Palo Alto, CA, USA).

3. Synthesis and characterization of functionalized hydrophobic nanocrystals

3.1. Synthesis of functionalized hydrophobic nanocrystals

As-prepared hydrophobic nanocrystals in their hydrophobic solvents (i.e., hexane or toluene) were precipitated by adding a polar solvent (i.e., isopropanol or acetone), transferred to THF, and adjusted to a concentration of 500 μg/mL. To a 250 μL aliquot of nanocrystal solution in THF were added 25 μL of amphiphilic oligonucleotide solutions in water with desired concentrations: 50, 250, 500, and 1000 μM. The reaction was conducted at room temperature while shaking at 500 rpm in a 0.5 mL Eppendorf tube for 2 h. After the reaction, modified nanocrystals were first collected by centrifuging the reaction mixture at 14000 rpm for 10 min, then washed 2 times with 200 μL water to remove excess amphiphilic DNA, and finally re-dispersed in either water or PBS for future use.

3.2. Characterization of functionalized hydrophobic nanocrystals

3.2.1. Determination of the number of ligand per functionalized hydrophobic nanocrystal

To determine the number of ligand per functionalized hydrophobic nanocrystal, fluorescently-labeled chimeric DNA molecules were used and their caliberation curves were first obtained by measuring their fluorescence intensity as a function of concentration. Then the fluorescence intensity of functionalized nanocrystals was measured and the ligand concentration of this sample was calculated out using previously obtained caliberation curve. Finally, the number of ligand per functionalized nanocrystal was calculated out by dividing the molar concentration of the ligand with the molar

concentration of the nanocrystal. All the fluorescence measurements were done on a fluorometer using a 100 µL cuvette.

3.2.2. TEM images of functionalized hydrophobic nanocrystals

TEM images of functionalized hydrophobic nanocrystals were obtained on the same instrument and using the same experimental conditions as specified in section 1.2. Since carbon film is hydrophobic and can cause false-negative nanocrystal aggregation, copper grids were first glow-discharged to become hydrophilic. Then 5 µL functionalized hydrophobic nanocrystals in water were dropped onto the treated copper grid, and the sample was air-dried at room temperature.

3.2.3. UV-Vis spectra of functionalized hydrophobic nanocrystals

UV-Vis spectra of unmodified nanocrystals in their hydrophobic solvents and modified nanocrystals in water were recorded on a Cary Bio-100 UV spectrometer (Varian, Palo Alto, CA, USA) using a 200 µL quartz cuvette.

3.2.4. Fourier transform infrared (FT-IR) spectra of functionalized hydrophobic nanocrystals

FT-IR spectra of vacuum-dried unmodified and modified nanocrystals were recorded on a Nicolet 6700 FT-IR spectrometer (Thermo Scientific, West Palm Beach, FL, USA) in KBr pellets.

3.2.5. Dynamic Light Scattering (DLS) measurement of functionalized hydrophobic nanocrystals

DLS data for functionalized hydrophobic nanocrystals in water were obtained on a ZetaPALS DLS detector (Brookhaven Instruments, Holtsville, NY, USA) at 25 ˚C using a 3 mL disposable cuvette. The scattering angle was fixed at 90˚.

4. Binding of functionalized hydrophobic nanocrystals with nucleic acid targets

Fe-Fe_3O_4 core-shell MNPs were functionalized with amphiphilic oligonucleotide (lipid-20 and lipid T20), as described in Section 2.1. Streptavidin-coated silica microspheres (SiMSs) (1 μm) were modified with complementary DNA (C-20). With a concentration of 10 mg/mL, the binding capacity of SiMSs to biotinylated molecules was 0.36 μM. Fifty μL as-purchased silica microspheres in buffer (100 mM borate, 10 mM EDTA, 1% BSA, 0.1% NaN_3, 0.05% Tween 20, pH = 8.5) were washed three times with hybridization buffer (10 mM Tris-HCl, 5 mM Mg^{2+}) and redispersed in 50 μL hybridization buffer. Then, 1 μL C-20 with a concentration of 500 μM was added to the washed silica microspheres, and the mixture was incubated while shaking for 1 h at room temperature. After the reaction, C-20-coated SiMSs were washed 3 times with hybridization buffer and redispersed in hybridization buffer. Following this, 50 μL functionalized MNPs with a concentration of 500 μg/mL were added to the washed DNA microspheres, and the mixture was incubated while shaking for 4h at room temperature to ensure maximal hybridization. After the reaction, MNP-coated silica SiMSs were collected by centrifuging at a very low speed (i.e., 1500 rpm) for 3 min, washed 3 times with hybridization buffer and redispersed in 100 μL hybridization buffer.

Scanning electron microcopy (SEM) images were obtained on an FE S-4000 scanning electron microscope (Hitachi, Tokyo). A 5.0-μL sample in hybridization buffer was spread on a piece of microglass slide mounted on a specimen stub using double-sided adhesive tape. The sample was then dried overnight in a desiccator, sputter coated with an ultrathin layer of gold, and then subjected to SEM imaging.

5. Binding of functionalized hydrophobic nanocrystals with cancer cell target

The Fe-Fe_3O_4 core-shell MNPs were functionalized with amphiphilic aptamer as described in Section 2.1. To demonstrate the specific interaction between amphiphilic aptamer-functionalized MNPs and cancer cells, fluorescence measurements were obtained on a FACScan cytometer (Becton Dickinson Immunocytometry Systems, San Jose, CA, USA) using a 488 nm laser as the excitation source. CEM or Ramos cells in culture medium were washed three times with washing buffer and then redispersed in binding buffer at a concentration of 10^6 cells/mL. To 200 μL CEM or Ramos cells in binding buffer, either aptamer alone or amphiphilic aptamer-functionalized MNPs with desired concentrations were added, and the mixture was incubated on ice for 30 min. The cells were washed three times with washing buffer, redispersed in binding buffer, and subjected to flow cytometry analysis by counting 10,000 events. For competitive inhabitation assay, cells were incubated with 1.5 μM unlabeled aptamer first and then follow the same procedures as normal binding assay.

6. Magnetic Resonance Imaging (MRI)

T_2-weighted MRI images were acquired on a 11 T/470 MHz MRI spectrometer (Bruker Optics, Billerica, MA). Amphiphilic aptamer-modified Fe-Fe_3O_4 core-shell MNPs were incubated with binding buffer only, CCRF-CEM cells, or Ramos cells in binding buffer on ice for 30 min in 500 μL binding buffer in 1.5 ml Eppendorf tubes. The final concentration for modified MNPs was 25 μg/mL, while the final concentration of cells was 10^6 cells/mL. After incubation, the samples in Eppendorf tubes were vortexed, fixed

on a homemade foam sample holder in a 1x3 array, and then put in the coil. T_2-weighted MRI images were acquired with a spin echo sequence.

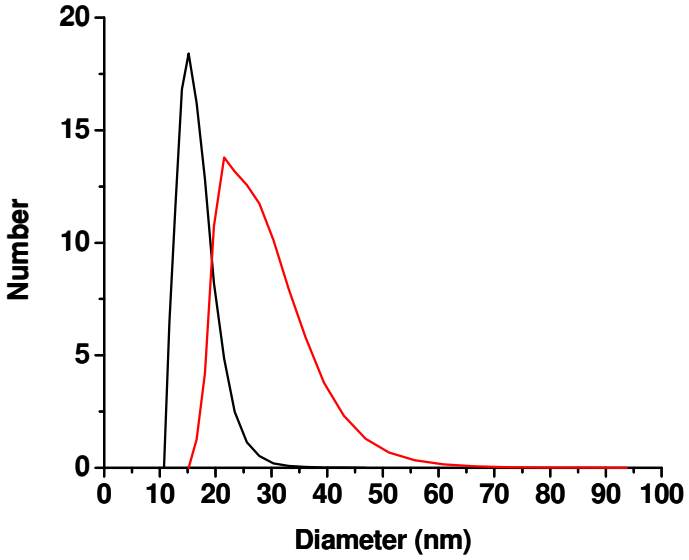

Figure S1. Dynamic light scattering (DLS) measurements of modified Fe-Fe_3O_4 CSNPs in water (red) and unmodified Fe-Fe_3O_4 CSNPs in hexane (black). Both unmodified and modified nanoparticles had a relatively narrow size distribution. In addition, the average diameter increase from 16.2 nm of unmodified nanoparticles to 27.2 nm of modified nanoparticles indicated a successful surface engineering. Lipid-T20 was used as the chimeric DNA molecule here.

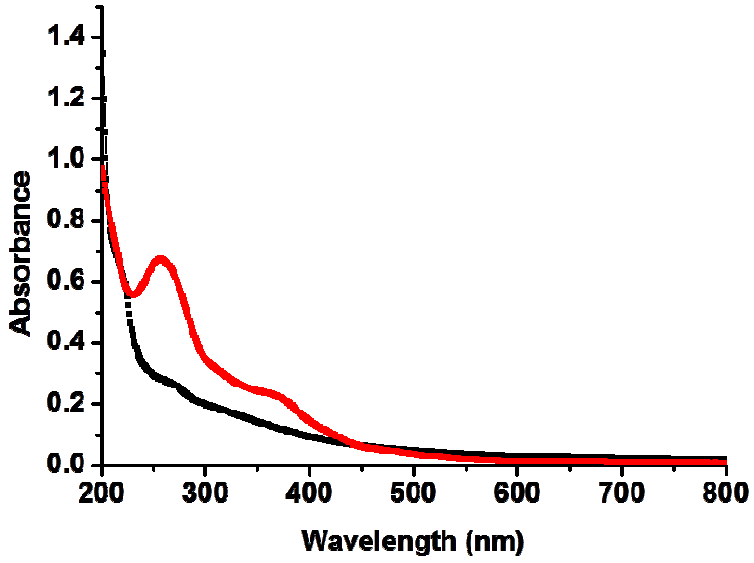

Figure S2. UV-Vis spectra of modified Fe-Fe_3O_4 CSNPs in water (red) and unmodified Fe-Fe_3O_4 CSNPs in hexane (black). The peak in the red curve is the characteristic absorption peak of DNA around 260 nm. Lipid-T20 was used as the chimeric DNA molecule here.

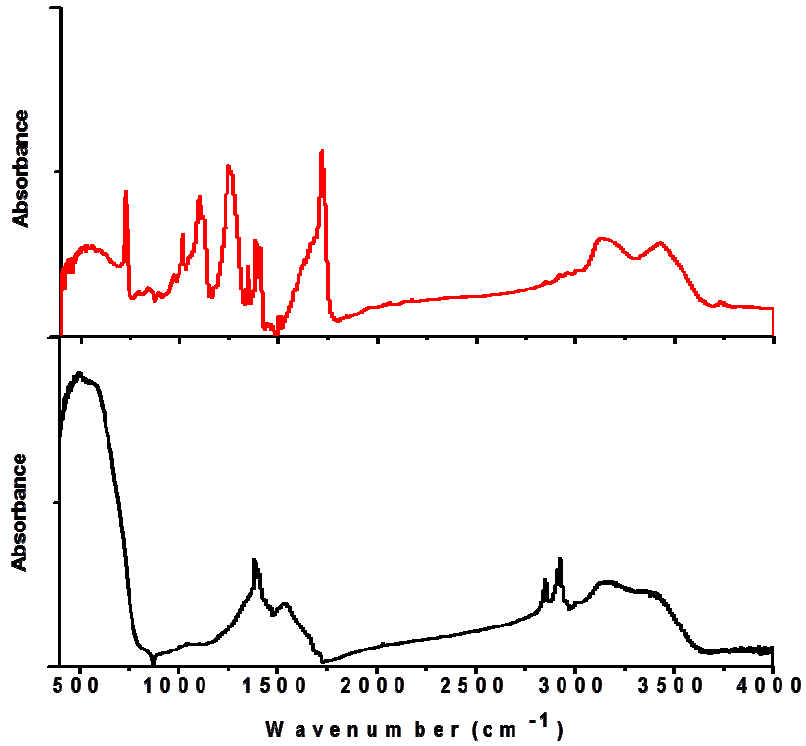

Figure S3. FT-IR spectra of modified (red) and unmodified (black) Fe-Fe_3O_4 CSNPs. Lipid-T20 was used as the chimeric DNA molecule here.

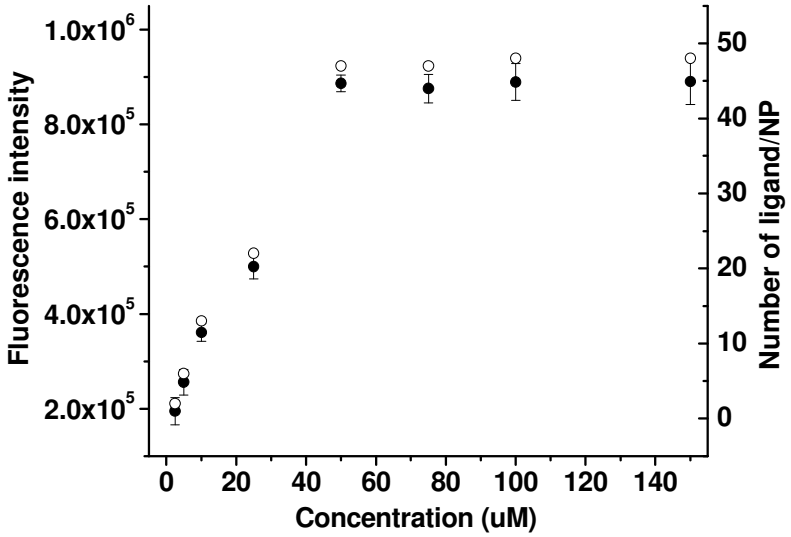

Figure S4. Fluorescence intensity and the number of ligand per engineered nanoparticle as a function of chimeric DNA molecule concentration for Fe-Fe_3O_4 CSNPs modified with lipid-T20.

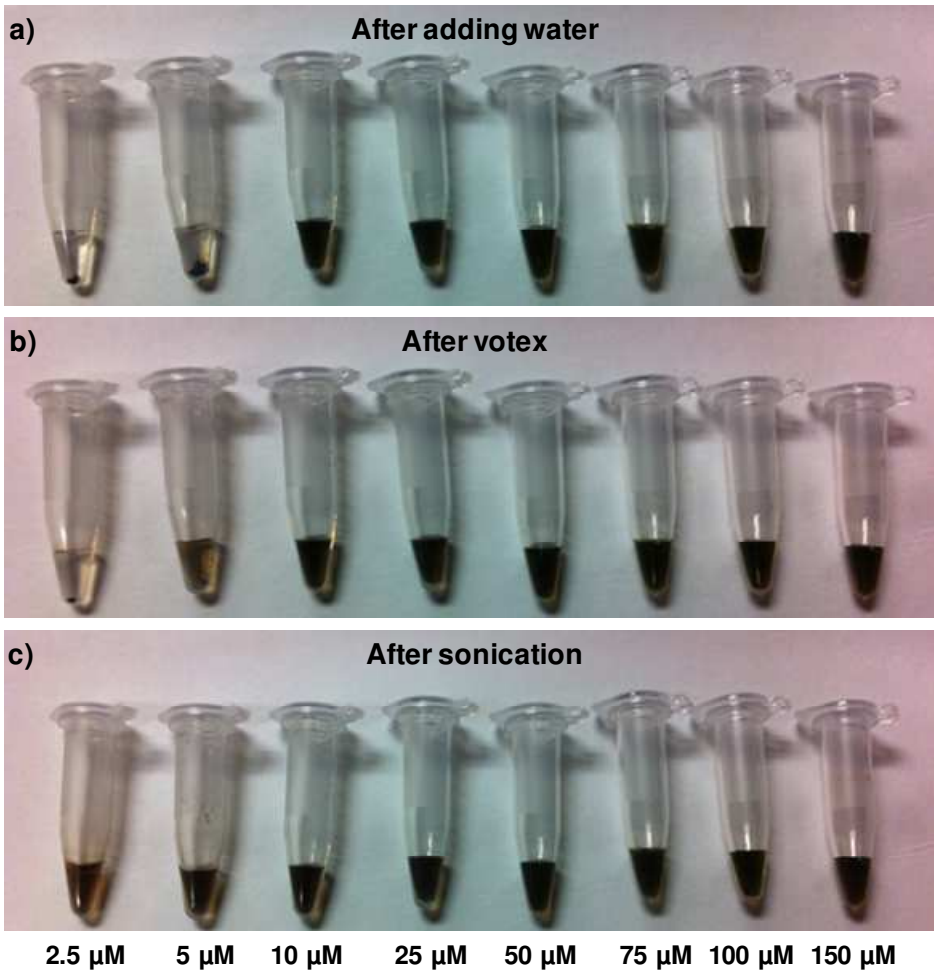

Figure S5. Fe-Fe_3O_4 CSNPs treated with different concentrations of lipid-T20. Fe-Fe_3O_4 CSNPs modified with adequate chimeric DNA molecules (≥ 10 µM) are soluble upon adding water (a), whereas these ones engineered with insufficient ligands need vigorous votex (5 µM) (b) or even sonication (2.5 µM) (c).

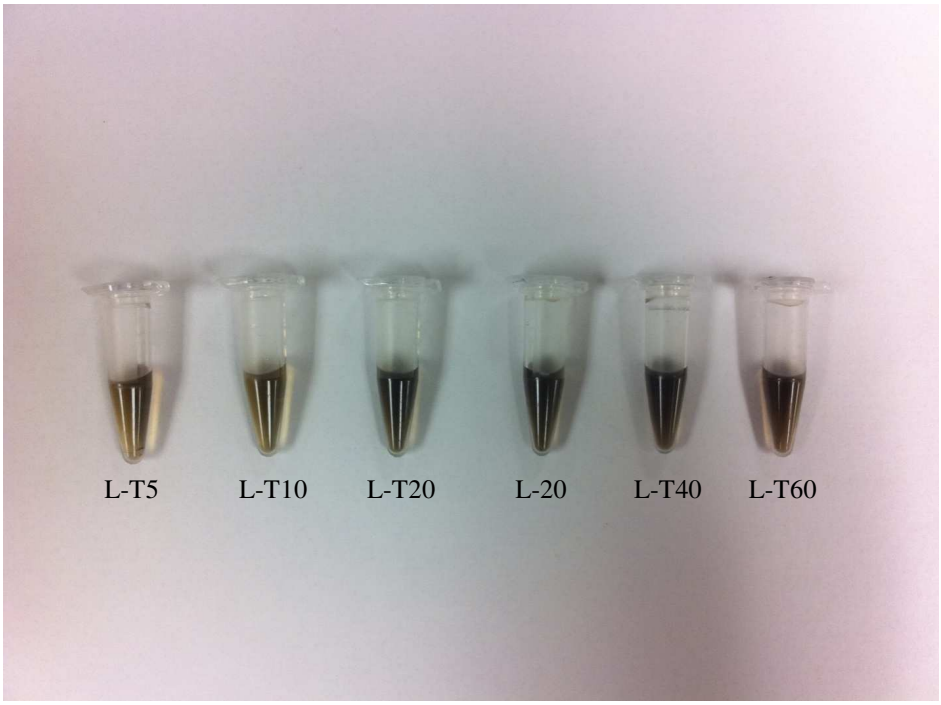

Figure S6. Fe-Fe_3O_4 CSNPs treated with amphiphilic oligonucleotide with different lengths and sequence information.

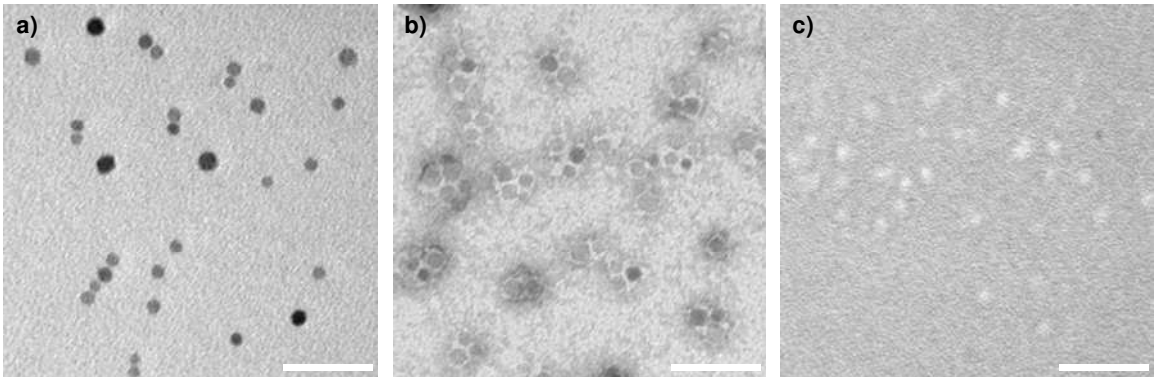

Figure S7. Transmission electron microscopy (TEM) images of (a) as-synthesized 7 nm Fe_3O_4 NPs in hexane, (b) lipid-T20 functionalized 7 nm Fe_3O_4 NPs in water, and (c) lipid-T20 only in water after negative staining by 2% uranyl acetate. With the negative staining technique, chimeric DNA molecules can be visualized as white circles in (b) or white dots in (c). Scale bar: 100 nm.

Table S1. Detailed sequence information and CPG selection for amphiphilic DNA.

Name	Sequence	CPG
Lipid-T5	5'-Lipid-TTT TT-3'	T
Lipid-T10	5'-Lipid-TTT TTT TTT T-3'	T
Lipid-T20	5'-Lipid-TTT TTT TTT TTT TTT TTT TT-3'	T
Lipid-T40	5'-Lipid-TTT TTT TTT TTT TTT TTT TTT TTT TTT TTT TTT TTT TTT T-3'	T
Lipid-T60	5'-Lipid-TTT TTT TTT TTT TTT TTT TTT TTT TTT TTT TTT TTT TTT TTT TTT TTT TTT TTT TTT TTT-3'	T
Lipid-20	5'-Lipid-TTA CTC GAG GGA TCC TAG TC-FITC-3'	FITC
cDNA	5'-Biotin-GAC TAG GAT CCC TCG AGT AA-3'	A
Lipid-PEG-Sgc8	5'-Lipid-$(PEG)_4$-ATC TAA CTG CTG CGC CGC CGG GAA AAT ACT GTA CGG TTA GA-FITC-3'	FITC
Sgc8	5'-ATC TAA CTG CTG CGC CGC CGG GAA AAT ACT GTA CGG TTA GA-3'	A

Table S2. Dynamic light scattering (DLS) and zeta-potential measurements of Fe-Fe_3O_4 CSNPs engineered with chimeric DNA molecules of different lengths and sequence information.

Name	Hydrodynamic diameter (nm)	Zeta-potential (mV)
Lipid-T5	19.3 ± 1.8	-9.76 ± 1.99
Lipid-T10	23.6 ± 1.4	-15.07 ± 0.71
Lipid-T20	27.2 ± 7.5	-30.17 ± 0.57
Lipid-20	28.1 ± 3.4	-29.55 ± 0.93
Lipid-T40	42.8 ± 0.3	-34.05 ± 1.32
Lipid-T60	55.9 ± 3.6	-40.30 ± 0.57

References

(1) Peng, S.; Wang, C.; Xie, J.; Sun, S. *J. Am. Chem. Soc.* **2006**, *128*, 10676-10677.

(2) Cheng, K.; Peng, S.; Xu, C.; Sun, S. *J. Am. Chem. Soc.* **2009**, *131*, 10637-10644.

(3) WangWang; Luo, J.; Fan, Q.; Suzuki, M.; Suzuki, I. S.; Engelhard, M. H.; Lin, Y.; Kim, N.; Wang, J. Q.; Zhong, C. J. *J. Phys. Chem. B* **2005**, *109*, 21593-21601.

(4) Wei, Y.; Klajn, R.; Pinchuk, A. O.; Grzybowski, B. A. *Small* **2008**, *4*, 1635-1639.

(5) Yang, Y.; Chen, O.; Angerhofer, A.; Cao, Y. C. *J. Am. Chem. Soc.* **2008**, *130*, 15649-15661.

(6) Xie, R.; Kolb, U.; Li, J.; Basché, T.; Mews, A. *J. Am. Chem. Soc.* **2005**, *127*, 7480-7488.

(7) Poudyal, N.; et al. *Nanotechnol.* **2008**, *19*, 355601.

(8) Lee, Y.; Garcia, M. A.; Frey Huls, N. A.; Sun, S. *Angew. Chem., Int. Ed*, **2010**, *49*, 1271-1274.

(9) Liu, H.; Zhu, Z.; Kang, H.; Wu, Y.; Sefan, K.; Tan, W. *Chem. -- Eur. J.* **2010**, *16*, 3791-3797.